

Oxidation State of Ce in CeO₂-Promoted Rh/Al₂O₃ Catalysts during Methane Steam Reforming: H₂O Activation and Alumina Stabilization

R. B. Duarte,[†] O. V. Safonova,[‡] F. Krumeich,[§] M. Makosch,[†] and J. A. van Bokhoven^{*,†,‡}

[†]ETH Zurich, Institute for Chemical and Bioengineering, 8093 Zurich, Switzerland

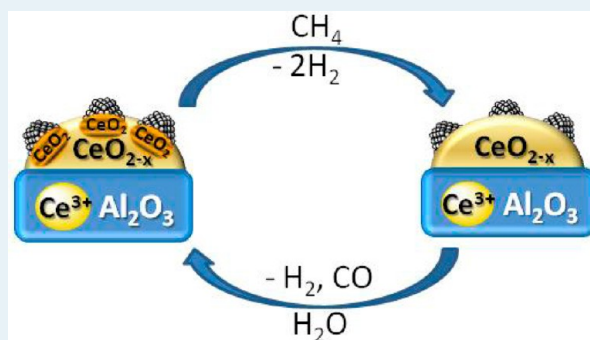
[‡]Paul Scherrer Institute, 5232 Villigen PSI, Switzerland

[§]ETH Zurich, Laboratory of Inorganic Chemistry, 8093 Zurich, Switzerland

S Supporting Information

ABSTRACT: The cerium oxidation state in ceria-doped Rh/Al₂O₃ catalysts during the methane steam reforming (MSR) reaction was determined by *in situ* X-ray absorption spectroscopy and online mass spectrometry at 773 K. The catalysts were characterized by electron microscopy and X-ray diffraction. The oxidation states of rhodium and cerium during MSR are related. A total of 25% of Ce⁴⁺ reduces to Ce³⁺ under a CH₄/H₂O/He flow when the catalyst is active in MSR (773 K). A slight reoxidation occurs when the catalyst is sequentially exposed to steam diluted in helium at high temperatures, showing that only a small fraction of CeO_{2-x} may be involved in the water activation step by reoxidation. The main role of ceria during reaction, besides the activation of water, is to stabilize the structure of alumina by forming CeAlO₃ and to maintain the dispersion of rhodium.

KEYWORDS: methane steam reforming, Rh/Al₂O₃ catalysts, CeO₂, Sm₂O₃, *in situ* X-ray absorption spectroscopy



1. INTRODUCTION

Catalysts containing ceria are extensively investigated, because they show unique catalytic performance based on their oxygen storage capacity (OSC). For example, three-way catalysts, which are used to control the gas exhaust from automobiles, have superior performance when promoted with ceria,¹ due to its OSC and the good interaction between ceria and precious metals. Ceria has the capacity to release and store oxygen by changing its oxidation state from Ce⁴⁺ to Ce³⁺ with a low redox potential. This property of ceria and CeO₂-containing materials was suggested to be useful in several reactions, like water-gas shift,^{2,3} CO oxidation,⁴ oxidation of hydrocarbons,^{5,6} and hydrogenation of organic compounds.⁷ Temperature programmed reduction profiles of ceria show two peaks, one at a low temperature (≈ 700 K) due to reduction at the surface and one at a high temperature (≈ 1100 K) which arises from bulk reduction.⁸ The presence of metal affects the ceria surface reduction process by accelerating it through H₂ spillover, which in turn affects the catalytic performance.^{9,10} Metal nanoparticles are highly stabilized when supported on ceria and have increased adhesion energy closer to oxygen defects.^{11,12} This strong interaction between CeO₂-modified Al₂O₃ and the metal phase stabilizes the small metal particles.^{13–15}

The methane steam reforming (MSR) reaction is the most important industrial technology for obtaining hydrogen.¹⁶ The catalysts used in industry are based on nickel¹⁷ because of its high activity and low price; however, they deactivate relatively

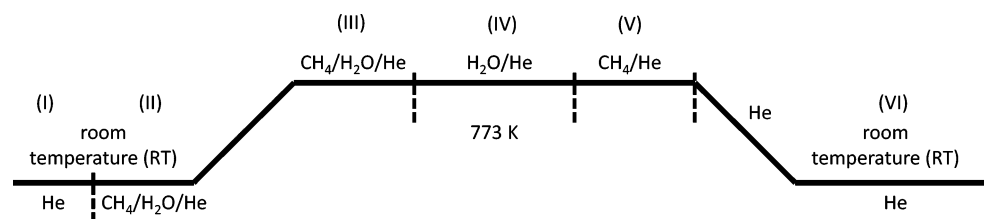
quickly. The addition of ceria as a promoter in Ni/Al₂O₃ catalysts improves their performance.^{18,19} Ceria is also efficient as a support and promoter for noble metal catalysts.^{15,20,21} Previous works reported that ceria activates water during MSR and helps to gasify carbon deposits, thus preventing deactivation.^{13,22,23} Craciun et al.²⁰ attributed the better performance of CeO₂-containing palladium catalysts to the redox properties of ceria, which leads to a reaction mechanism where oxygen from ceria reacts with dissociated methane on the precious metal. The presence of the Ce⁴⁺/Ce³⁺ redox couples increases the methane conversion and carbon resistance also over platinum catalysts.¹³ Halabi et al.²² proposed a mechanism for Rh/Ce_{0.6}Zr_{0.4}O₂ catalysts in which methane dissociatively adsorbs on the Rh active sites and steam on ceria. Kundakovic et al.²⁴ observed that the reactivity of ceria depends on its reduction degree. In Rh/CeO₂, the dissociation of water happens only in the presence of Ce³⁺; however it is not clear whether it proceeds on Rh, on CeO_{2-x}, or at their interface. The presence of rhodium in reduced ceria promotes water dissociation and the formation of hydrogen at lower temperatures. Padeste et al.²⁵ showed that the reducibility of ceria depends on its crystallinity and the capability of activating water depends on its reduction degree. In contrast, a DFT

Received: March 19, 2013

Revised: July 5, 2013

Published: July 8, 2013

Scheme 1. Treatment Related to XANES Measurement in Figure 1



study on the interaction of CeO₂ (111) surfaces with water shows that its dissociation is favored at room temperature in both oxidized and reduced ceria surfaces.²⁶ Previous studies report that the support does not relevantly influence any kinetic reaction step in MSR, but that it only influences the dispersion of the active phase.^{27–29}

γ -Al₂O₃ is widely used as a catalyst support, and it undergoes phase transitions and sintering under hydrothermal treatment, which is delayed by the addition of rare earth oxides.³⁰ The modification of γ -Al₂O₃ by lanthana was more effective than that by ceria for improving its thermal resistance. The addition of La³⁺ to a Pt/CeO₂/Al₂O₃ system prevents the alumina phase transitions during hydrothermal treatment.³¹ The addition of metal oxides to the CeO₂-containing support can also increase its OSC.³² The incorporation of La³⁺ into CeO₂ leads to the formation of more anionic oxygen vacancies and consequentially improves the performance of Pt/CeO₂-Al₂O₃ catalysts.¹³ Sm₂O₃ and La₂O₃ have similar structures, and both can be incorporated into CeO₂, causing large changes in the support properties.³³ The addition of Sm₂O₃ to a CeO₂-Al₂O₃ support improves the activity and stability of platinum and rhodium catalysts with nanoscale dispersion during methane reforming reactions.^{14,15}

The enhanced performance of the CeO₂-containing samples is often suggested to be related to the reversible changing oxidation state of cerium. Insights into the influence of ceria on the catalyst stability and on the reaction mechanism can be obtained by determining the catalyst structure and electronic properties during reaction. *In situ* X-ray absorption spectroscopy (XAS) combined with online mass spectrometry³⁴ can provide this information.³⁵ X-ray absorption near edge structure (XANES) spectroscopy yields the averaged cerium oxidation state and can be applied under *in situ* conditions. Spectral deconvolution yields the quantitative amount of the various components.³⁶ Elfallah et al.³⁷ studied the redox process of CeO₂ and Rh/CeO₂ using XAS at the Ce L₃-edge, and a quantitative analysis of the oxidation state was performed under different treatments. The degree of ceria reduction as function of temperature was also measured by Overbury et al.³⁸ using XANES measurements at the Ce L₃-edge. The addition of zirconium increases the extent of cerium reduction while rhodium accelerates the reduction process, causing it to occur at lower temperatures. A combination of X-ray spectroscopy at Ce K and L edges allowed quantification of the oxidation states of polyhedral CeO₂ nanoparticles of different sizes under ambient conditions.³⁹ Our work aims to determine the oxidation state of cerium in Rh/CeO₂-Sm₂O₃-Al₂O₃ catalysts under MSR conditions to clarify its structure, oxidation state, and role in the MSR reaction mechanism employing online MS, *in situ* XAS, and *ex situ* electron microscopy and X-ray diffraction.

2. EXPERIMENTAL SECTION

2.1. Catalyst Preparation. γ -Al₂O₃ was prepared via sol-gel synthesis⁴⁰ by mixing Al(OC₄H₉sec)₃ with 6.5 mol of ethanol and water at 333 K. The gel formed was stirred for 1 h, and a solution of 25 mL of HNO₃ (0.11 mol/L) was added. The obtained mixture was stirred for 14 h under reflux. The gel was then dried at room temperature (RT) and calcined at 773 K for 6 h under synthetic air. CeO₂-Al₂O₃ and CeO₂-Sm₂O₃-Al₂O₃ oxide supports were prepared by wetness impregnation of the sol-gel γ -Al₂O₃. Appropriate quantities of Ce(NO₃)₃·6H₂O and Sm(NO₃)₃·6H₂O were dissolved in ethanol and added to γ -Al₂O₃. The mixture was stirred for 5 h at room temperature and dried at 333 K in a roto-evaporator under vacuum conditions. The resulting powder was dried at 373 K for 12 h and then calcined at 1223 K for 6 h. The 12CeO₂-Al₂O₃ support had a theoretical CeO₂ content of 12 wt %, and 6CeO₂-6Sm₂O₃-Al₂O₃ contained 6 wt % of each oxide. Rh catalysts supported on the mixed CeO₂-Sm₂O₃-Al₂O₃ oxides were obtained by wet impregnation of the supports with a solution of RhCl₃ (20%) in ethanol as described above. The samples were dried at 373 K and calcined at 773 K under air for 12 and 4 h, respectively. The amount of Rh was measured with Inductively Coupled Plasma-Optical Emission Spectrometry (ICP-OES) in a VISTA AX spectrometer (Varian, Agilent Technologies), and the value is about 0.5 wt %.

2.2. Sample Characterization. The 12CeO₂-Al₂O₃ support and the respective Rh catalyst were characterized by scanning transmission electron microscopy (STEM). The measurements were performed with the aberration-corrected dedicated STEM microscope HD 2700 CS (Hitachi, acceleration potential of 200 kV).⁴¹ A high-angle annular dark-field (HAADF) detector was used to produce images with atomic number (Z) contrast. An energy-dispersive X-ray spectrometer (EDXS; from EDAX) was attached to the microscope and used for EDXS analyses. X-ray diffraction (XRD) patterns were collected with an X'PERT PRO-MPD diffractometer with Cu K α radiation and a Ni filter and were recorded in a 2 θ range, from 10° to 70°, at intervals of 0.02 for 2 s. The ceria particle size of the catalysts after calcination at 773 K was estimated using the Scherrer equation.⁴²

2.3. In Situ XAS Measurements. XAS measurements at the Ce L₃ edge were performed at the superXAS beamline at the Swiss Light Source, Villigen, Switzerland.⁴³ Energy scans were performed with a Si (111) channel cut monochromator. Spectra were collected in fluorescence mode using a germanium detector. XANES spectra were recorded from 5.660 to 5.820 keV. The experimental setup consisted of a fixed bed 0.8 mm capillary reactor with a wall thickness of 0.01 mm heated by a gas blower oven.⁴⁴ A mass spectrometer was plugged on line for analysis of the products. The XAS experiments were performed at different steps of the treatment (Scheme 1): the catalysts were exposed to He at room temperature and then to an atmosphere of 2.3 mL/min of 5%

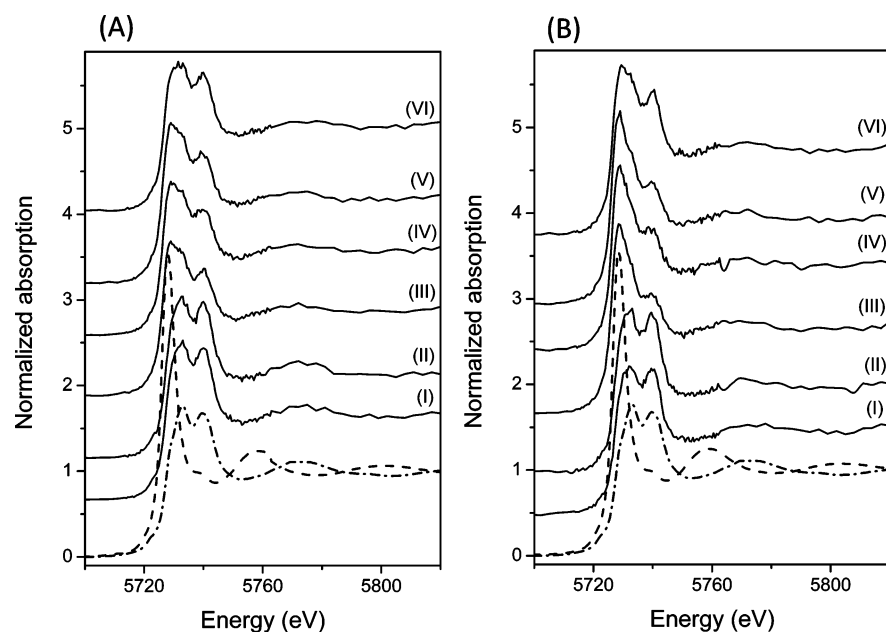


Figure 1. *In situ* Ce L_3 -edge normalized XANES spectra of Rh/12CeO₂-Al₂O₃ (A) and Rh/6CeO₂-6Sm₂O₃-Al₂O₃ (B) at each step of the treatment indicated in Scheme 1. Spectra are offset along the ordinate for clarity. Dashed line and dash-dotted line are reference spectra of Ce³⁺ (of Ce(NO₃)₃) and Ce⁴⁺ (of CeO₂), respectively.

CH₄/He and 10 mL/min of He through a water saturator yielding a ratio of H₂O/CH₄ of 3. Water was degassed with He prior to the experiment. The temperature was ramped up until 773 at 5 K/min. Under these conditions, the Rh/12CeO₂-Al₂O₃ catalyst presented a reaction rate of 1.2 molecules_{CH₄} site⁻¹ s⁻¹ and the Rh/6CeO₂-6Sm₂O₃-Al₂O₃ catalyst a rate of 1.6 molecules_{CH₄} site⁻¹ s⁻¹. At 773 K, the atmosphere was switched between H₂O and CH₄, both diluted in He, with dwells of 45 min while collecting the XANES spectra. A flow of pure He was used in the cooling step. Another experiment was carried out where the Rh/12CeO₂-Al₂O₃ catalyst was heated up under He to 773 K and a flow of H₂O diluted in He was maintained at 773 K for 45 min. The acquisition time of one spectrum was 6 min. The raw XAS data were background corrected and normalized using the Athena software package.⁴⁵ The traces for CO, CO₂, H₂, O₂, H₂O, and CH₄ were recorded by the mass spectrometer and were divided by the helium signal for normalization.

3. RESULTS

3.1. Qualitative Study of the Ce Oxidation State.

Scheme 1 shows the treatment applied to the catalysts during the XAS experiments, the data of which are depicted in Figure 1. Initially the catalysts were exposed to He at room temperature (I). The atmosphere was then switched to 1 kPa CH₄, 3 kPa H₂O, 100 kPa total pressure, and balance He (II). The temperature was increased to 773 at 5 K/min (III). At 773 K, the atmosphere was changed to H₂O diluted in He (IV) and then to CH₄ diluted in He (V). A flow of pure He (5 ppmv O₂ and 5 ppmv H₂O impurity) was used in the cooling step (VI).

Figure 1 shows the Ce L_3 -edge XANES spectra of Rh/12CeO₂-Al₂O₃ (A) and Rh/6CeO₂-6Sm₂O₃-Al₂O₃ (B) measured under different gas compositions and temperatures. The indicated numbers correspond to the steps in Scheme 1. Reference spectra of Ce³⁺ (Ce(NO₃)₃, dashed line) and Ce⁴⁺ (CeO₂, dash-dotted line) are also given. The spectrum of Ce³⁺ is dominated by one intense feature at around 5.70 keV. The

edge position of the spectrum of Ce⁴⁺ is shifted to higher energy and two main features 5 eV apart of about the same intensity are apparent. The spectra of Rh/12CeO₂-Al₂O₃ at room temperature, both under an atmosphere of He and CH₄/H₂O/He (conditions I and II in Scheme 1), show a shape characteristic of cerium in the completely oxidized state. At 773 K (condition III) the spectrum shows an increase in the white line intensity and an edge-shift to lower energy, indicating that Ce⁴⁺ partially reduces to Ce³⁺. We previously showed that rhodium is mainly oxidized under CH₄/H₂O/He at RT, and it gets practically completely reduced when active during MSR¹⁵ (Figure S1 in Supporting Information). When the sample was subsequently exposed to diluted H₂O (condition IV), only tiny changes are observed in the spectrum, which means that only a small fraction changed oxidation state. After the flow was switched to CH₄ diluted in He (condition V) again only marginal changes were observed. The spectra under CH₄/H₂O/He and CH₄/He at 773 K were virtually overlapping. The spectrum measured at RT after the different treatments (condition VI) enhanced the features of the completely oxidized cerium, but with a slight decreased second maximum compared to the initial spectrum, revealing the tendency to incomplete reoxidation upon cooling, which likely happens due to residual oxygen in the helium flow. The changes in the promoter oxidation state accompany the changes observed for rhodium¹⁵ (Figure S1 in Supporting Information). The Sm₂O₃-containing sample (Figure 1B) shows the same trend under the conditions applied. At 773 K (conditions III, IV, and V), the spectra show a more intense and narrow white line, indicating a higher extent of ceria reduction compared to the Rh/12CeO₂-Al₂O₃ catalyst.

Figure 2 shows the Ce L_3 -edge XANES spectra taken under He at RT and under He, respectively, H₂O/He at 773 K over Rh/12CeO₂-Al₂O₃. The changing between He and H₂O/He atmospheres at high temperatures was done in sequence. As mentioned before, the XANES spectrum of Rh/12CeO₂-Al₂O₃ under He at RT shows exclusively features that are character-

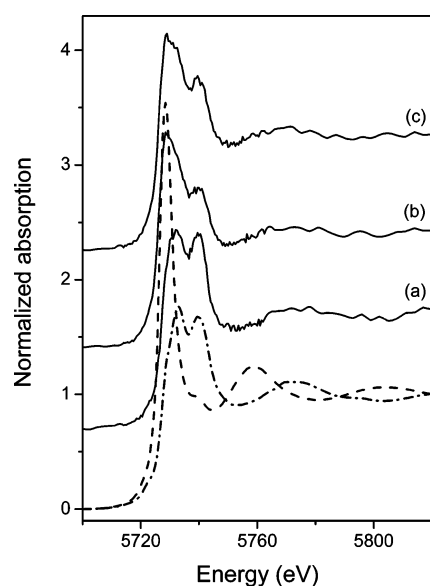


Figure 2. *In situ* Ce L₃-edge normalized XANES spectra of Rh/12CeO₂-Al₂O₃: (a) He at RT, (b) He at 773 K, (c) H₂O/He at 773 K. Spectra are offset along the ordinate for clarity. Dashed line and dash-dotted line are reference spectra of Ce³⁺ (of Ce(NO₃)₃) and Ce⁴⁺ (of CeO₂), respectively.

istic of Ce⁴⁺. At 773 K under He, the spectrum shows the same trend as when it was heated up under a CH₄/H₂O/He atmosphere: a partial reduction from Ce⁴⁺ to Ce³⁺ happens. Ceria shows a tendency to autoreduce to CeO_{2-x}. The spectrum taken after the change to H₂O/He flow, shows a slight decrease in intensity of the white line, which means that again a tiny amount of reoxidation occurred.

3.2. Quantitative Study of the Ce Oxidation State. A linear combination analysis of the XANES spectra was done using the reference spectra of Ce(NO₃)₃ and CeO₂ to obtain the fractions of Ce⁴⁺ and Ce³⁺ at different stages of the treatment (Table 1). The initial concentration of Ce⁴⁺ in the catalysts is 100%, under both He and CH₄/H₂O/He at RT (conditions I and II). Partial reduction of cerium occurs at high temperatures (conditions III, IV and V). The presence of Sm₂O₃ facilitates the reduction of cerium: under CH₄/H₂O/He, only 57% of the cerium remains in the Ce⁴⁺ state in Rh/6CeO₂-6Sm₂O₃-Al₂O₃ while 75% in Rh/12CeO₂-Al₂O₃. The exposure of partially reduced ceria to H₂O/He at high temperature (condition IV) leads to reoxidation of a few percent of Ce³⁺, which is at the border of the accuracy of our measurements ($\approx 1\%$). The small increase is consistent for both samples, whenever exposed to water. This suggests that a low number of cerium atoms undergo a redox change: only a small amount of CeO_{2-x} is involved in the water activation mechanism by reoxidation. After switching the atmosphere to CH₄/He (condition V), the amount of reduced cerium is the same as in condition III. Again the change was small, but the trend observed for both samples was the same. After cooling to room temperature (condition VI), a partial reoxidation occurs. The presence of Sm₂O₃ in the support hinders this reoxidation: about 46% of Ce³⁺ in Rh/6CeO₂-6Sm₂O₃-Al₂O₃ reoxidizes versus 56% in Rh/12CeO₂-Al₂O₃. The quantitative evaluation done for Rh/12CeO₂-Al₂O₃ shows that autoreduction of ceria happens when the catalyst is heated under He up to 773 K. The amount of Ce⁴⁺ in this case (72%) is close to the value obtained when the sample is heated under CH₄/H₂O/He (75%). The

Table 1. Quantitative Oxidation State of Cerium in CeO₂-Doped Catalysts under Differential Catalytic and Controlled Conditions

sample	atmosphere	condition ^a	temperature (K)	fraction Ce ⁴⁺
Rh/12CeO ₂ -Al ₂ O ₃	He	I	298	1
	CH ₄ /H ₂ O/He ^b	II	298	1
	CH ₄ /H ₂ O/He	III	773	0.75
	H ₂ O/He	IV	773	0.77
	CH ₄ /He	V	773	0.75
	He (after reaction)	VI	298	0.89
Rh/6CeO ₂ -6Sm ₂ O ₃ -Al ₂ O ₃	He	I	298	0.98
	CH ₄ /H ₂ O/He	II	298	0.98
	CH ₄ /H ₂ O/He	III	773	0.57
	H ₂ O/He	IV	773	0.60
	CH ₄ /He	V	773	0.57
	He (after reaction)	VI	298	0.77
Rh/12CeO ₂ -Al ₂ O ₃	He	-	298	1
	He	-	773	0.72
	H ₂ O/He	-	773	0.75

^aConditions relate to Scheme 1. ^b1 kPa CH₄, 3 kPa H₂O, 100 kPa total pressure, balance He.

small increase in the quantity of Ce⁴⁺ when exposed to H₂O/He again is consistent for all samples.

3.3. Characterization: STEM, EDXS, and XRD. Figure 3 shows an HAADF-STEM micrograph of the Rh/12CeO₂-Al₂O₃ catalyst after reduction under 5%H₂/He at 773 K for 1 h and the EDX spectra of two indicated areas. Individual rhodium and ceria particles are difficult to distinguish from their contrast as both show up bright in the Z contrast micrograph while the light alumina support is gray ($Z_{\text{Ce}} = 58$; $Z_{\text{Rh}} = 45$ vs $Z_{\text{Al}} = 13$). The large bright patches in the center of the image correspond to ceria crystals with a diameter of ca. 10 nm. For determining the composition of the smaller particles with diameters in the range of 1–3 nm, EDXS spot analyses have been performed. Area 1 shows a low rhodium signal, a more intense cerium signal, and a high aluminum signal, revealing that these elements are present in the same area. The EDX spectrum of area 2 shows intense rhodium and aluminum peaks and no cerium.

Figure 4 shows typical HAADF-STEM micrographs of the 12CeO₂-Al₂O₃ support after calcination at 1223 K for 6 h (top) and after reduction at 773 K for 1 h (bottom). After calcination, ceria is present as crystals with diameters between ca. 2 and 5 nm. The thermal treatment in H₂ leads to the formation of larger particles and highly dispersed cerium. An analysis of the size of the larger particles is difficult due to agglomeration, but the distinguishable particles have sizes between ca. 4 and 10 nm. At higher magnification, the presence of bright spots reveals that many small CeO_x clusters or even single Ce atoms are present besides the ceria crystals.

Figure 5A shows the XRD patterns of the γ -Al₂O₃ support after calcination at 773 K for 6 h and the Rh/12CeO₂-Al₂O₃ catalyst after calcination at 773 K for 4 h and after MSR reaction at 1033 K for 2 h. The XRD pattern of ceria with a fluorite type structure is added as a reference. Reflections of ceria are visible at $2\theta = 28.6^\circ$, 33.1° , 47.5° , and 56.1° . Those of

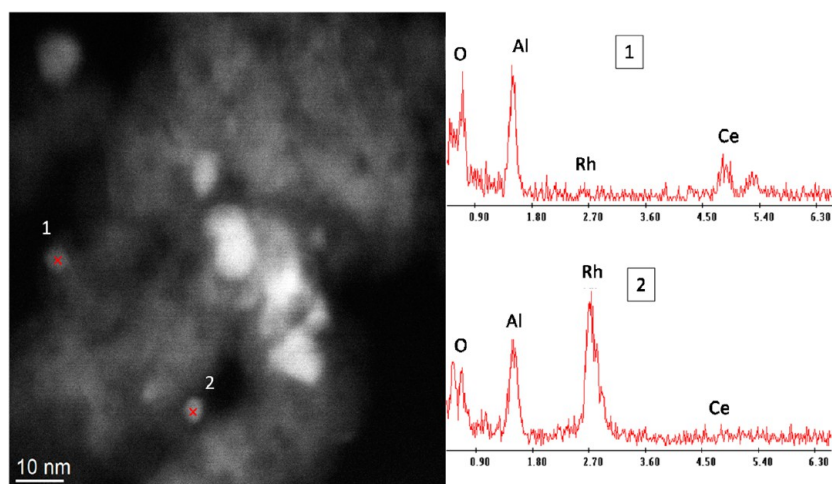


Figure 3. HAADF-STEM micrograph of Rh/12CeO₂-Al₂O₃ catalyst after reduction at 773 K for 1 h and EDX spectra of the indicated areas.

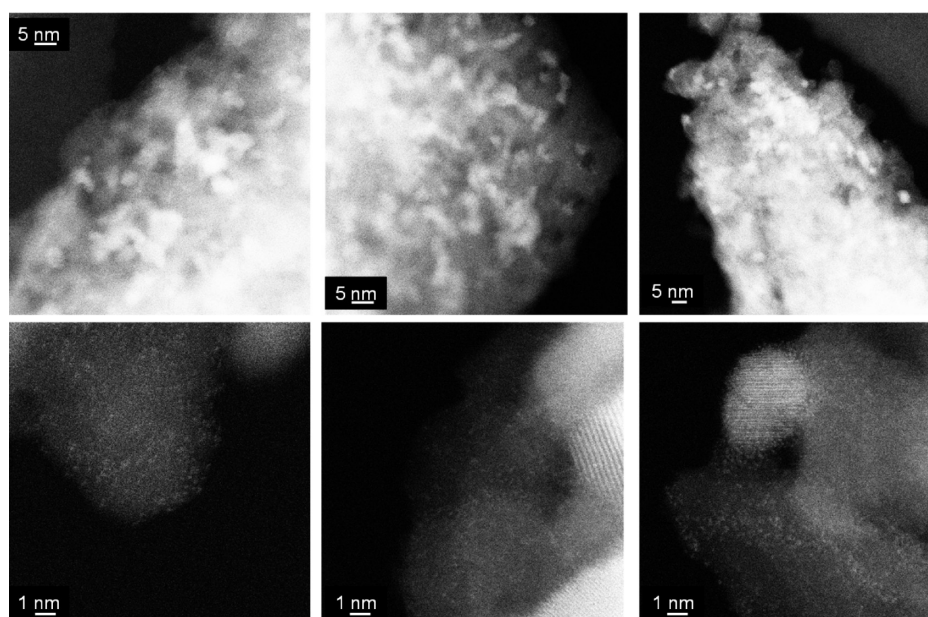


Figure 4. HAADF-STEM micrographs of 12CeO₂-Al₂O₃ support after calcination at 1223 K for 6 h (top) and after reduction at 773 K for 1 h (bottom). Cerium appears as bright spots and bright areas (Z contrast).

alumina are at $2\theta = 37.5^\circ$, 39.4° , and 45.6° . The relative intensity of the lines of ceria compared to those of alumina decreased after MSR reaction. Figure 5B shows the XRD patterns of the Rh/6CeO₂-6Sm₂O₃-Al₂O₃ catalyst after calcination at 773 K and after MSR reaction at 1033 K. Due to the lower ceria content, the diffraction lines attributed to ceria are much less intense in comparison to Rh/12CeO₂-Al₂O₃. Estimation of the ceria particle size using the Scherrer equation shows that the addition of samarium oxide to the support does not cause changes in the ceria particle size when compared to the ceria-containing support. Both Rh/12CeO₂-Al₂O₃ and Rh/6CeO₂-6Sm₂O₃-Al₂O₃ catalysts after calcination at 773 K show an average particle size of 3.1 nm. After MSR, the relative intensities of the ceria reflections were again decreased when compared to the alumina peaks.

4. DISCUSSION

Ce L₃-edge XANES spectra taken under different conditions show that the redox state of cerium is a function of temperature

and atmosphere. Cerium after preparation is fully oxidized under He and CH₄/H₂O/He atmospheres (conditions I and II in Scheme 1). Partial reduction of ceria occurs with heating. Thermodynamic data provide information on the oxygen binding energies of ceria, and the surface energies are much lower than those associated with the bulk.^{12,46} The amount of Ce³⁺ depends on the presence of other components in the catalyst (Table 1). The Sm₂O₃-containing catalyst shows a higher quantity of Ce³⁺ species ($\approx 43\%$) at high temperatures than Rh/12CeO₂-Al₂O₃ ($\approx 25\%$). The XRD patterns of the catalysts after calcination at 773 K show that the ceria particles have roughly the same size in both samples, therefore the higher degree of reduction in the Rh/6CeO₂-6Sm₂O₃-Al₂O₃ sample is probably due to the ability of Sm₂O₃ to stabilize Ce³⁺. The defects in CeO_{2-x} are oxygen vacancies, and ceria doping with oxides of metals with lower valencies may create more vacancies.⁴⁷ Studies on the water-gas shift reaction over Pt/Ce_xZr_{1-x}O₂ catalysts showed that the introduction of Zr⁴⁺ into the ceria lattice decreases the Ce⁴⁺ to Ce³⁺ reduction energy.⁴⁸

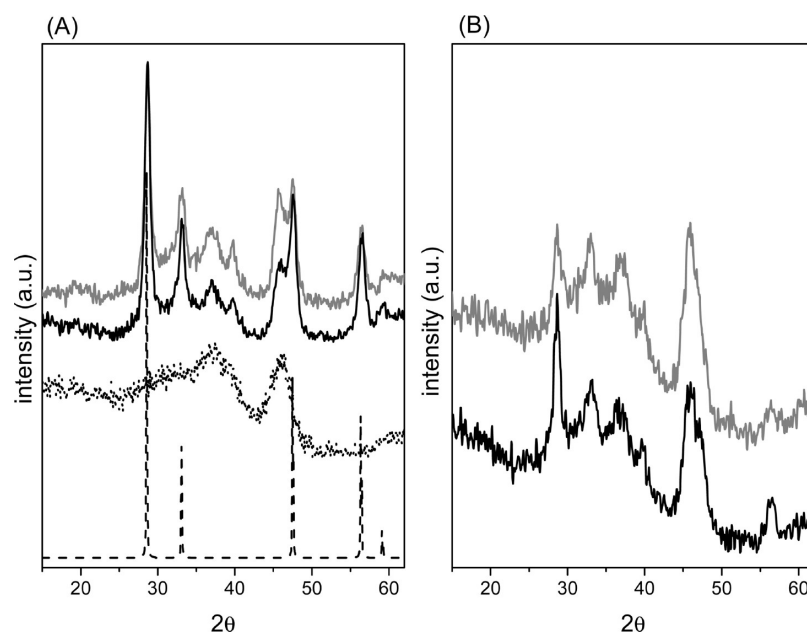


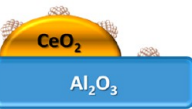
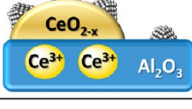
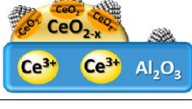
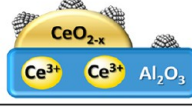
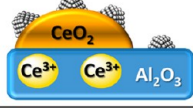
Figure 5. XRD patterns of the catalysts: (A) Rh/12CeO₂-Al₂O₃ and (B) Rh/6CeO₂-6Sm₂O₃-Al₂O₃ after calcination at 773 K for 4 h (black lines) and after MSR reaction at 1033 K for 2 h (gray lines). The dashed line indicates the pattern of CeO₂ with a fluorite-type structure, and the dotted line corresponds to the XRD pattern of the γ -Al₂O₃ support after calcination at 773 K for 6 h.

Previous XAS experiments of Rh/ x Sm₂O₃- y CeO₂-Al₂O₃ catalysts at the Rh K-edge showed that rhodium changes its oxidation state from oxidic to reduced when active in MSR at 773 K.¹⁵ The same behavior is observed for cerium, which partially reduces to Ce³⁺. CeO₂ has a high oxygen mobility compared to other oxides such as Al₂O₃, SiO₂, ZrO₂, and MgO,⁴⁹ and the reducibility of cerium under MSR conditions suggests that it may participate actively in the reaction mechanism. Recent works^{22,23} reported that the mechanism of MSR, when carried out on Rh/CeO₂-containing catalysts, involves two distinct sites: rhodium active metal sites perform the CH₄ dissociation while steam is dissociatively adsorbed on CeO₂. CeO₂, when partially reduced, was reported to reoxidize when in contact with H₂O, producing H₂.^{24–26,50} The quantitative XANES analysis of both samples under a flow of H₂O/He at 773 K (condition IV) shows that only a few percent of CeO_{2- x} gets reoxidized. As the exposure to He only did not lead to this reoxidation, we concluded that the water is responsible for the reoxidation. After cooling, a higher fraction of Ce³⁺ reoxidizes, which indicates that a higher fraction of cerium is able to do a redox than actually occurs under the influence of water at high temperatures. The oxidation of CeO_{2- x} by steam is endothermic and was reported to occur at mild temperatures (\approx 500 K).^{50,51} It is facilitated in the presence of noble metals.^{24,50,52} Kundakovic et al.²⁴ found that CeO_{2- x} activates H₂O and gets oxidized upon H₂ desorption. H₂ desorption starts at 500 K, and it is facilitated by rhodium, but the water activation only depends on the cerium oxidation state. The reducibility of ceria was reported to depend on its specific surface area and crystallinity, but once capable of reducing, it should get oxidized under water flow.²⁵ Elfallah et al.³⁷ studied the redox properties of pure CeO₂ and Rh/CeO₂, and they found that rhodium facilitates the surface reduction of ceria due to the faster H₂ dissociation. However, it hampers the oxidation reaction. The trend observed for both our samples to undergo very little reoxidation under H₂O/He flow reveals that the oxidation state of only a fraction of Ce³⁺ is affected by the

water-containing atmosphere and suggests that only this fraction is able to activate water and participate in the mechanism under the conditions used in this study by performing a redox activation. We observed that part of the rhodium is in contact with ceria (Figure 3). The rhodium clean surface was reported to not dissociate water; however, in the presence of boron its adsorptive properties dramatically change, causing water activation.⁵³ The interactions that exist in the complex catalytic system make it difficult to uncover where each mechanistic step of the MSR reaction proceeds, notably the water activation. It is not clear if the water activation involving CeO_{2- x} proceeds on Rh, with a spillover of oxygen, onto CeO_{2- x} or directly at the metal–support interface. The absence of water activation on the bare metal suggests that the metal–support interface may play a decisive role. Vayssilov et al.¹² found through DFT calculations that at high temperatures (>500 K) the reducibility of ceria nanoparticles in contact with metal is due to oxygen spillover and the Ce³⁺ centers migrate to the more stable positions, which include the metal–ceria boundary and deeper ceria layers. The subsequent exposure of the catalysts to a CH₄/He flow caused rereduction of the small amount of reoxidized cerium, indicative of the reactivity of the formed oxygen.

When cooled under helium, both samples show significant but incomplete reoxidation of CeO_{2- x} . The presence of small amounts of oxygen in the helium flow causes reoxidation. However, this process is not complete, and only part of Ce³⁺ reverts back to Ce⁴⁺. Piras et al.⁵⁴ performed redox treatments in CeO₂-promoted Al₂O₃ and also observed that part of the Ce³⁺ formed under reductive treatment did not reoxidize after exposure to oxidizing conditions. This behavior was attributed to incorporation of the Ce³⁺ in the Al₂O₃ structure with the formation of CeAlO₃. The cerium that does not show reoxidation is likely present in such a phase, which may be responsible for the stabilization of alumina.¹⁵ Figure S2 in Supporting Information shows that the spectrum of CeAlO₃ closely resembles that of the reference Ce³⁺ spectrum, which

Table 2. Proposed Mechanism Based on STEM, EDXS, XRD, and *in Situ* XANES for the Behavior of Ceria during Different Steps of Treatment and Quantitative Oxidation State of Ce³⁺ in the Catalysts under the Different Conditions^a

Proposed mechanism (● Rh ⁰ and ● Rh ³⁺)	Ce ³⁺ (%)			
	Rh/12CeO ₂ -Al ₂ O ₃		Rh/6CeO ₂ -6Sm ₂ O ₃ -Al ₂ O ₃	
	In CeO _{2-x}	In Al ₂ O ₃	In CeO _{2-x}	In Al ₂ O ₃
He at RT 	0	0	2	0
CH ₄ /H ₂ O/He at 773K 	14	11	20	23
H ₂ O/He at 773K 	12	11	17	23
CH ₄ /He at 773K 	14	11	20	23
He (O ₂) at RT 	0	11	0	23

^aReactive conditions cause partial reduction of Ce⁴⁺. Part of the Ce³⁺ function is to stabilize the alumina. A minor part of Ce³⁺ is involved in water activation.

thus provides spectroscopic support of Ce³⁺ in CeAlO₃. The STEM images of the 12CeO₂-Al₂O₃ support after reduction at 773 K for 1 h show CeO₂ particles and bright spots representing cerium atoms. The dispersed cerium in the images may be incorporated into the alumina support. Additionally, the XRD patterns of samples after MSR at high temperature show significantly suppressed ceria peaks, in agreement with conversion of part of the crystalline ceria into a different phase, probably embedded in the alumina matrix.⁵⁵ Shyu et al.⁵⁶ observed the formation of CeO_{2-x} when CeO₂-Al₂O₃ was treated under H₂ at 873 K and the formation of CeAlO₃ after longer heating. CeO_{2-x} species reoxidized when exposed to air at RT while CeAlO₃ showed good thermal stability in air in the temperature range up to 873 K in agreement with our data. Ferreira et al.⁵⁷ observed, through XPS measurements, a high concentration of Ce³⁺ species in a 12CeO₂-Al₂O₃ support, which were stabilized by interaction with alumina, also after thermal treatment under air at high temperatures. It was reported⁵⁷ that after reductive treatment at higher temperatures, cerium was mainly present as Ce³⁺. When heated under a flow of pure He up to 773 K, reduction of part of the ceria also happens. The formation of CeAlO₃ was previously reported to happen even after oxidative treatment in a Pt/CeO₂-Al₂O₃ system,⁵⁸ and the Ce³⁺ species were stable under O₂ at 1173 K.

Table 2 shows a proposed mechanism based on the XANES, STEM, EDXS and XRD. The quantitative results for Ce³⁺

obtained from the linear combination analysis of the XANES spectra are also shown. After preparation and at room temperature, Rh₂O₃ particles are sitting on alumina and on ceria, which is present as CeO₂. In the presence of Sm₂O₃, 2% of cerium is Ce³⁺. Under a MSR atmosphere at 773 K, rhodium gets fully reduced (Figure S1 in Supporting Information) while only part of the ceria changes its oxidation state from Ce⁴⁺ to Ce³⁺. The Ce³⁺ is partially present in the CeO_{2-x} particle and partially embedded in the Al₂O₃ matrix. The exposure of the catalysts to a H₂O/He flow led to the reoxidation of a few percent of the Ce³⁺. With the change of the atmosphere to CH₄/He, the same small fraction rereduced. After cooling to room temperature under a helium flow containing traces of oxygen, the Ce³⁺ species which are present in the CeO_{2-x} particle get reoxidized while the other part of the Ce³⁺ is stabilized by alumina and remains Ce³⁺.

5. CONCLUSIONS

During methane steam reforming at 773 K over Rh/CeO₂-Al₂O₃ catalysts (promoted or not with Sm₂O₃), the oxidation states of cerium and rhodium are related.¹⁵ The oxidation state of cerium under active catalytic conditions in MSR is partially reduced and that of rhodium completely. Only a small fraction of Ce³⁺ was reoxidized when the catalysts were exposed to steam-containing flow, indicating the participation of this Ce³⁺ in water activation causing its reoxidation. These Ce⁴⁺ atoms are readily reduced to Ce³⁺ after reacting with methane,

indicating their reactivity. The presence of Sm_2O_3 in the support leads to a higher extent of ceria reduction at high temperatures and to the retention of a greater amount of reducibles after cooling to room temperature. A significant fraction of Ce^{3+} incorporates into alumina forming CeAlO_3 species. Ceria as a promoter for $\text{Rh}/\text{Al}_2\text{O}_3$ catalysts under MSR conditions at 773 K, besides its activity for H_2O activation, has the main role of stabilizing the alumina structure by forming CeAlO_3 and by maintaining the dispersion of the active phase.¹³

■ ASSOCIATED CONTENT

■ Supporting Information

In situ Rh K-edge normalized XANES spectra of $\text{Rh}/12\text{CeO}_2\text{-Al}_2\text{O}_3$ under different conditions. This material is available free of charge via the Internet at <http://pubs.acs.org>.

■ AUTHOR INFORMATION

Corresponding Author

*Phone: +41 44 632 55 42. E-mail: jeroen.vanbokhoven@chem.ethz.ch

Notes

The authors declare no competing financial interest.

■ ACKNOWLEDGMENTS

The Swiss Light Source at the Paul Scherrer Institute, Villigen, Switzerland, is acknowledged for the use of its facilities at the SuperXAS beamline.

■ REFERENCES

- (1) Kim, G. *Ind. Eng. Chem. Prod. Res.* **1982**, *21*, 267.
- (2) Bunluesin, T.; Gorte, R. J.; Graham, G. W. *Appl. Catal., B* **1998**, *15*, 107.
- (3) Hilaire, S.; Wang, X.; Luo, T.; Gorte, R. J.; Wagner, J. *Appl. Catal., A* **2001**, *215*, 271.
- (4) Bharali, P.; Saikia, P.; Reddy, B. M. *Catal. Sci. Technol.* **2012**, *2*, 931.
- (5) Liu, W.; Flytzani-Stephanopoulos, M. *J. Catal.* **1995**, *153*, 304.
- (6) Zamar, F.; Trovarelli, A.; Deleitenburg, C.; Dolcetti, G. *J. Chem. Soc., Chem. Commun.* **1995**, 965.
- (7) Vivier, L.; Duprez, D. *ChemSuschem* **2010**, *3*, 654.
- (8) Trovarelli, A.; Dolcetti, G.; Deleitenburg, C.; Kaspar, J. *Stud. Surf. Sci. Catal.* **1993**, *75*, 2781.
- (9) Trovarelli, A. *Catal. Rev.* **1996**, *38*, 439.
- (10) Sadi, F.; Duprez, D.; Gerard, F.; Miloudi, A. *J. Catal.* **2003**, *213*, 226.
- (11) Farmer, J. A.; Campbell, C. T. *Science* **2010**, *329*, 933.
- (12) Vayssilov, G. N.; Lykhach, Y.; Migani, A.; Staudt, T.; Petrova, G. P.; Tsud, N.; Skala, T.; Bruix, A.; Illas, F.; Prince, K. C.; Matolin, V.; Neyman, K. M.; Libuda, J. *Nat. Mater.* **2011**, *10*, 310.
- (13) Mortola, V. B.; Damyanova, S.; Zanchet, D.; Bueno, J. M. C. *Appl. Catal., B* **2011**, *107*, 221.
- (14) Duarte, R. B.; Damyanova, S.; de Oliveira, D. C.; Marques, C. M. P.; Bueno, J. M. C. *Appl. Catal., A* **2011**, *399*, 134.
- (15) Duarte, R. B.; Nachtegaal, M.; Bueno, J. M. C.; van Bokhoven, J. A. *J. Catal.* **2012**, *296*, 86.
- (16) Holladay, J. D.; Hu, J.; King, D. L.; Wang, Y. *Catal. Today* **2009**, *139*, 244.
- (17) Rostrup-Nielsen, J. R.; Sehested, J.; Norskov, J. K. *Adv. Catal.* **2002**, *47*, 65.
- (18) Dan, M.; Lazar, M. D.; Rednic, V.; Almasan, V. *Rev. Roum. Chim.* **2011**, *56*, 643.
- (19) Rakib, A.; Gennequin, C.; Dhainaut, T.; Ringot, S.; Aboukais, A.; Abi-Aad, E. *Adv. Mater. Res. (Durten-Zurich, Switz.)* **2011**, *324*, 153.
- (20) Craciun, R.; Shereck, B.; Gorte, R. J. *Catal. Lett.* **1998**, *51*, 149.
- (21) Feio, L. S. F.; Hori, C. E.; Damyanova, S.; Noronha, F. B.; Cassinelli, W. H.; Marques, C. M. P.; Bueno, J. M. C. *Appl. Catal., A* **2007**, *316*, 107.
- (22) Halabi, M. H.; de Croon, M. H. J. M.; van der Schaaf, J.; Cobden, P. D.; Schouten, J. C. *Appl. Catal., A* **2010**, *389*, 80.
- (23) Halabi, M. H.; de Croon, M. H. J. M.; van der Schaaf, J.; Cobden, P. D.; Schouten, J. C. *Appl. Catal., A* **2010**, *389*, 68.
- (24) Kundakovic, L.; Mullins, D. R.; Overbury, S. H. *Surf. Sci.* **2000**, *457*, 51.
- (25) Padeste, C.; Cant, N. W.; Trimm, D. L. *Catal. Lett.* **1993**, *18*, 305.
- (26) Watkins, M. B.; Foster, A. S.; Shluger, A. L. *J. Phys. Chem. C* **2007**, *111*, 15337.
- (27) Jones, G.; Jakobsen, J. G.; Shim, S. S.; Kleis, J.; Andersson, M. P.; Rossmelisl, J.; Abild-Pedersen, F.; Bligaard, T.; Helveg, S.; Hinnemann, B.; Rostrup-Nielsen, J. R.; Chorkendorff, I.; Sehested, J.; Norskov, J. K. *J. Catal.* **2008**, *259*, 147.
- (28) Lighthart, D. A. J. M.; van Santen, R. A.; Hensen, E. J. M. *J. Catal.* **2011**, *280*, 206.
- (29) Wei, J. M.; Iglesia, E. *J. Phys. Chem. B* **2004**, *108*, 4094.
- (30) Chongheng, H. e.; Yanglong, G.; Ren, W. *Shiyu Huagong* **1998**, *27*.
- (31) Usmen, R. K.; Graham, G. W.; Watkins, W. L. H.; McCabe, R. W. *Catal. Lett.* **1995**, *30*, 53.
- (32) Campbell, C. T.; Peden, C. H. F. *Science* **2005**, *309*, 713.
- (33) Hormes, J.; Pantelouris, M.; Balazs, G. B.; Rambabu, B. *Solid State Ionics* **2000**, *136*, 945.
- (34) De Vos, D. E.; Dams, M.; Sels, B. F.; Jacobs, P. A. *Chem. Rev.* **2002**, *102*, 3615.
- (35) Singh, J.; Lamberti, C.; van Bokhoven, J. A. *Chem. Soc. Rev.* **2010**, *39*, 4754.
- (36) Bordiga, S.; Groppo, E.; Agostini, G.; van Bokhoven, J. A.; Lamberti, C. *Chem. Rev.* **2013**, *113*, 1736.
- (37) Elfallah, J.; Boujana, S.; Dexpert, H.; Kiennemann, A.; Majerus, J.; Touret, O.; Villain, F.; Lenormand, F. *J. Phys. Chem.* **1994**, *98*, 5522.
- (38) Overbury, S. H.; Huntley, D. R.; Mullins, D. R.; Glavee, G. N. *Catal. Lett.* **1998**, *51*, 133.
- (39) Paun, C.; Safonova, O. V.; Szlachetko, J.; Abdala, P. M.; Nachtegaal, M.; Sa, J.; Klymenov, E.; Cervellino, A.; Krumeich, F.; van Bokhoven, J. A. *J. Phys. Chem. C* **2012**, *116*, 7312.
- (40) Vazquez, A.; Lopez, T.; Gomez, R.; X, B. *J. Mol. Catal., A* **2001**, *167*, 91.
- (41) Krumeich, F.; Muller, E.; Wepf, R. A.; Nesper, R. *J. Phys. Chem. C* **2011**, *115*, 1080.
- (42) Jones, F. W. *Proc. R. Soc. London, Ser. A* **1938**, *166*, 0016.
- (43) Abdala, P. M.; Safonova, O. V.; Wiker, G.; van Beek, W.; Emerich, H.; van Bokhoven, J. A.; Sa, J.; Szlachetko, J.; Nachtegaal, M. *Chimia* **2012**, *66*, 699.
- (44) van Beek, W.; Safonova, O. V.; Wiker, G.; Emerich, H. *Phase Transitions* **2011**, *84*, 726.
- (45) Newville, M. *J. Synchrotron Radiat.* **2001**, *8*, 322.
- (46) Zhou, G.; Shah, P. R.; Montini, T.; Fornasiero, P.; Gorte, R. J. *Surf. Sci.* **2007**, *601*, 2512.
- (47) Mogensen, M.; Sammes, N. M.; Tompsett, G. A. *Solid State Ionics* **2000**, *129*, 63.
- (48) Kalamaras, C. M.; Dionysiou, D. D.; Efstathiou, A. M. *ACS Catal.* **2012**, *2*, 2729–2742.
- (49) Martin, D.; Duprez, D. *J. Phys. Chem.* **1996**, *100*, 9429.
- (50) Otsuka, K.; Hatano, M.; Morikawa, A. *J. Catal.* **1983**, *79*, 493.
- (51) Gorte, R. J. *AIChE J.* **2010**, *56*, 1126.
- (52) Song, Z. X.; Nishiguchi, H.; Liu, W.; Yamada, H.; Takami, A.; Kudo, K.; Nagaoka, K.; Takita, Y. *Catal. Lett.* **2006**, *111*, 169.
- (53) Kiss, J.; Solymosi, F. *Surf. Sci.* **1986**, *177*, 191.
- (54) Piras, A.; Trovarelli, A.; Dolcetti, G. *Appl. Catal., B* **2000**, *28*, L77.
- (55) Damyanova, S.; Perez, C. A.; Schmal, M.; Bueno, J. M. C. *Appl. Catal., A* **2002**, *234*, 271.

- (56) Shyu, J. Z.; Weber, W. H.; Gandhi, H. S. *J. Phys. Chem.* **1988**, *92*, 4964.
- (57) Ferreira, A. P.; Zanchet, D.; Rinaldi, R.; Schuchardt, U.; Damyanova, S.; Bueno, J. M. C. *Appl. Catal., A* **2010**, *388*, 45.
- (58) Pitchon, V.; Zins, J. F.; Hilaire, L.; Maire, G. *React. Kinet. Catal. Lett.* **1996**, *59*, 203.